Chromosoma (2007) 116:29–40
DOI 10.1007/s00412-006-0078-0

RESEARCH ARTICLE

Human chromosomal bands: nested structure, high-definition map and molecular basis

Maria Costantini · Oliver Clay · Concetta Federico · Salvatore Saccone · Fabio Auletta · Giorgio Bernardi

Received: 7 July 2006 / Accepted: 15 August 2006 / Published online: 28 October 2006

Abstract In this paper, we report investigations on the nested structure, the high-definition mapping, and the molecular basis of the classical Giemsa and Reverse bands in human chromosomes. We found the rules according to which the ~3,200 isochores of the human genome are assembled in high (850-band) resolution bands, and the latter in low (400-band) resolution bands, so forming the nested mosaic structure of chromosomes. Moreover, we identified the borders of both sets of chromosomal bands at the DNA sequence level on the basis of our recent map of isochores, which represent the highest-resolution, ultimate bands. Indeed, beyond the 100-kb resolution of the isochore map, the guanine and cytosine (GC) profile of DNA becomes turbulent owing to the contribution of specific sequences such as exons, introns, interspersed repeats, CpG islands, etc. The isochore-based level of definition (100 kb) of chromosomal bands is much higher than the cytogenetic definition level (2–3 Mb). The major conclusions of this work concern the high degree of order found in the structure of chromosomal bands, their mapping at a high definition, and the solution of the long-standing problem of the molecular basis of chromosomal bands, as these could be defined on the basis of compositional DNA properties alone.

Communicated by S. Henikoff

Electronic supplementary material Supplementary material is available for this article at http://dx.doi.org/10.1007/s00412-006-0078-0 and is accessible for authorized users.

M. Costantini · O. Clay · F. Auletta · G. Bernardi (✉)
Laboratory of Molecular Evolution,
Stazione Zoologica Anton Dohrn,
80121 Naples, Italy
e-mail: bernardi@szn.it

C. Federico · S. Saccone
Dipartimento di Biologia Animale "M. La Greca",
University of Catania,
95124 Catania, Italy

Introduction

Almost 40 years ago, two experimental approaches opened the way to a better understanding of the genome organization of eukaryotes. The first was the quinacrine staining of metaphase chromosomes (Caspersson et al. 1968, 1970), which was shown to produce cross bands. This method allowed, for the first time, the identification of individual human chromosomes via their specific banding patterns, and was followed by the development of other banding methods. The most popular of these relied on treating metaphase chromosomes with dyes after proteolytic digestion or heat denaturation (Dev et al. 1972), and produced G bands (Giemsa-positive or Giemsa dark bands, which are essentially equivalent to the original Q bands or quinacrine bands) and R bands (Reverse bands, which are essentially equivalent to Giemsa-negative or Giemsa light bands).

The second experimental approach was ultracentrifugation in Cs_2SO_4 density gradients in the presence of sequence-specific ligands (e.g., Ag^+), which provided a high-resolution fractionation of mammalian DNA according to base composition (Corneo et al. 1968). The latter approach showed that the genomes of warm-blooded vertebrates are characterized by a striking long-range compositional heterogeneity (Filipski et al. 1973; Thiery et al. 1976). Indeed, these genomes are mosaics of isochores (Macaya et al. 1976), long (>>300 kb), compositionally fairly homogeneous DNA regions, which belong to a small number of families [L1, L2, H1, H2, H3, in order of increasing guanine and cytosine ratio (GC)]. These families are characterized by different base compositions

and, as observed later, by different structural and functional properties, such as gene density, replication timing, and chromatin structure (see Bernardi 2004 for a review).

The two sets of results led us to propose a correlation between the GC-poor and GC-rich isochores with G and R bands, respectively (Cuny et al. 1981). Our arguments were the following: (a) There were indications that Caspersson's chromosomal bands were related to base composition of DNA because quinacrine fluoresces with AT-rich DNA (Weisblum and de Haseth 1972; Ellison and Barr 1972; Pachmann and Rigler 1972; Comings 1978). (b) G bands were very evident in warm-blooded but much less so in cold-blooded vertebrates (Bailly et al. 1973; Stock and Mengden 1975; Schmid 1978); likewise, the genome of the former showed a much stronger compositional heterogeneity compared to that of the latter (Thiery et al. 1976). (c) G bands were highly conserved in birds (Stock and Mengden 1975) and mammals (Dutrillaux et al. 1975; Wurster-Hill and Gray 1979) as were the isochores of these genomes (Thiery et al. 1976). (d) Isochore size was compatible with the average amount of DNA per band, at the highest resolutions of up to 3,000 bands that were reported by Yunis (1976, 1981) and Yunis et al. (1977). (e) Gene amplification led to the formation of "homogeneous staining regions" in chromosomes (for a review, see Schimke 1982), the result expected if the amplified genome segments were smaller in size than isochores, which was the case.

The proposal of Cuny et al. (1981) was confirmed by a number of later results (Bernardi 1989): (a) G bands are 3.2% GC poorer than R bands (Holmquist et al. 1982); (b) G bands replicate late, R bands replicate early (Comings 1978), as did genes previously investigated in replication timing (Furst et al. 1981; Goldman et al. 1984) and localized in those bands; (c) genes are preferentially located in R bands (Goldman et al. 1984; Korenberg and Engels 1978), as well as in GC-rich isochores (Bernardi et al. 1985); (d) genes located in G and R bands are GC-poor and GC-rich, respectively (Aota and Ikemura 1986; Ikemura and Aota 1988), as are genes located in GC-poor and GC-rich isochores (Bernardi et al. 1985); (e) G bands can be produced by Hae III degradation of metaphase chromosomes (Lima-de-Faria et al. 1980), as expected from the fact that the GGCC sites split by Hae III are much more frequent in GC-rich compared to GC-poor isochores, whereas R bands can be produced by pancreatic DNase degradation of chromosomes protected by GC-specific binding of chromomycin A3 (Schweizer 1977). It was stressed, however (Bernardi 1989), that the general correlation between GC-poor/GC-rich isochores and G/R chromosomal bands could only be considered an approximation of the actual situation, because GC-rich (H1, H2, H3) and GC-poor (L1, L2) DNA components in the human genome are in a 1:2 ratio, whereas R and G bands are in a 1:1 ratio.

A further step was made by compositional mapping (Bernardi 1989). Compositional maps could be constructed by assessing GC levels around landmarks (e.g., genes localized on the physical maps) that could be probed. Because of the mosaic isochore structure of the mammalian genome, this simply required hybridizing the probes on compositional DNA fractions as obtained from density gradient centrifugation, or assessing GC levels of physically mapped DNA as cloned in YACs (yeast artificial chromosomes), for example. Compositional maps allowed us to first measure isochores, and we found that they ranged from 0.2 Mb for a very GC-rich isochore (De Sario et al. 1996) to more than 6 Mb for a very GC-poor isochore (De Sario et al. 1997). Incidentally, these values happen to essentially coincide with the extremes of the isochores' size distribution as determined by recent work (Costantini et al. 2006). Other compositional maps were obtained by hybridizing DNA fractions from the GC-poorest L1 and the GC-richest H3 isochore families (after suppressing the contribution of repetitive DNA) on metaphase (400-band resolution), prometaphase (850-band resolution) and interphase chromosomes (Saccone et al. 1992, 1993, 1996, 1999, 2002; Federico et al. 2000).

In this paper, we report on the structure of the human chromosomal bands, as investigated at 400-band (or low) resolution, at 850-band (or high) resolution and at the isochore (or highest) resolution, and on their mapping at the highest resolution of 100 kb. On the basis of these results, we could reach a conclusion on the long-standing problem of the molecular basis of chromosomal banding.

Materials and methods

Band nomenclature and conventions used For the low-resolution bands (400-band level), we used the definitions of ISCN (1981). For the high-resolution bands (850-band level) we used the idiogram of Francke (1994). The definitions, assignments, and recommended resolutions of bands have changed several times since the 1971 Conference (see The National Foundation 1972, Bostock and Sumner 1978 for idiograms), in particular at the 300–400 band level. For example, the original definition regarded 1p36 as a single band, whereas the ISCN 1981 Convention for 400 bands split 1p36 into three bands (1p36.1, 1p36.2, and 1p36.3; see, for example, Rooney 2001, pp. 263–267). These three bands are now even retained for the 300-band classification chosen by ISCN (2005), at the expense of fusing the originally distinct bands 1q22, 1q23, and 1q24 on the same chromosome.

Furthermore, the current conventions are, in turn, being questioned and may need to be reassessed (Lehrer et al. 2004; Claussen et al. 2005). Under these circumstances, we

decided to follow the classical (ISCN 1981) choice of bands at the 400-band level, which has remained essentially unchanged during the past 25 years.

It is important to point out that our conclusions do not depend sensitively on the differences among conventions for low-resolution bands. Indeed, we make use of those bands only to demonstrate the assembly rules, which are general, and to estimate how often each of those rules is used (see Table S3), but not for mapping or calculating length statistics, which are both done at the 850-band level.

Results

Nomenclature and compositional mapping of cytogenetic bands As several of our previous results and conventions concerning chromosomal bands are used in this paper, we briefly summarize them here. As shown in Table 1, at a low (400-band) resolution, G bands (as defined by ISCN 1981; see also Materials and methods) can be subdivided into two classes of bands, $L1^+$ and $L1^-$, according to whether they do or do not hybridize single-copy DNA from the GC-poorest L1 family. On the other hand, low (400-band) resolution R bands (as defined by Dutrillaux and Lejeune 1971) can be subdivided into three classes of bands according to their hybridization of single-copy DNA from the GC-richest isochore families H2–H3: we called $H3^+$, H3*, and $H3^-$ the R bands that showed a strong, a weak, and no hybridization, respectively (Saccone et al. 1992, 1993, 1996). The relationship with the classes of R bands described by Dutrillaux (1973) and Holmquist et al. (1982) will be presented in a following section.

At the high resolution of 850 bands, G bands can be subdivided in $L1^+$ and $L1^-$ bands according to the same criterion used for low-resolution bands (see above). The correspondence with the four staining intensities of G bands (Francke 1994) will be presented in a later section. Likewise, at this resolution, R bands could be classified into just two sets: those that hybridized to H3 DNA, the $H3^+$ bands; and those that did not, the $H3^-$ bands (Saccone et al. 1996, 1999, 2002; see Fig. 1). We indicate by "G_{400}, R_{400}" and "G_{850}, R_{850}" the Giemsa and Reverse bands as obtained at low (400-band) and high (850-band) resolutions, respectively.

Table 1 summarizes not only the results obtained by isochore hybridization on human chromosomes and the

Table 1 Chromosomal bands as defined by isochore hybridization

			Approximate equivalence	Amount %	Average GC[8]	SD GC[9]
At 400 band resolution:						
		L1 hybridization				
G bands	$L1^+$	Present				
	$L1^-$	Absent				
		H3 hybridization				
R bands	$H3^+$	Strong[1]	T bands[2]			
	H3*	Weak[3,4,5]				
	$H3^-$	Absent[3,4,5]	"Mundane"[6]			
At 850 band resolution:						
		L1 hybridization				
G bands	$L1^+$	Present[5]	G1, G2[7]	13.4	36.3	1.09
	$L1^-$	Absent[5,10]	G3, G4[7]	34.4	40.1	2.88
				47.8		
		H3 hybridization				
R bands	$H3^-$	Absent[10,11]		37.4	41.5	2.75
	$H3^+$	Present[10,11]		14.8	47.7	3.03
				52.2		

[1] Saccone et al. 1992
[2] T bands are the temperature-resistant T(elomeric) bands of Dutrillaux (1973).
[3] H3* bands were previously designated as R* (Saccone et al. 1993).
[4] Saccone et al. 1996
[5] Federico et al. 2000
[6] Holmquist 1992
[7] G1, G2, G3, and G4 are our designations for the four classes of G bands of decreasing staining intensity described by Francke (1994).
[8] GC is the molar ratio of guanine and cytosine in DNA.
[9] SD is the standard deviation of GC.
[10] $H3^-$ and $L1^-$ bands are also called intermediate bands.
[11] Saccone et al. 1999

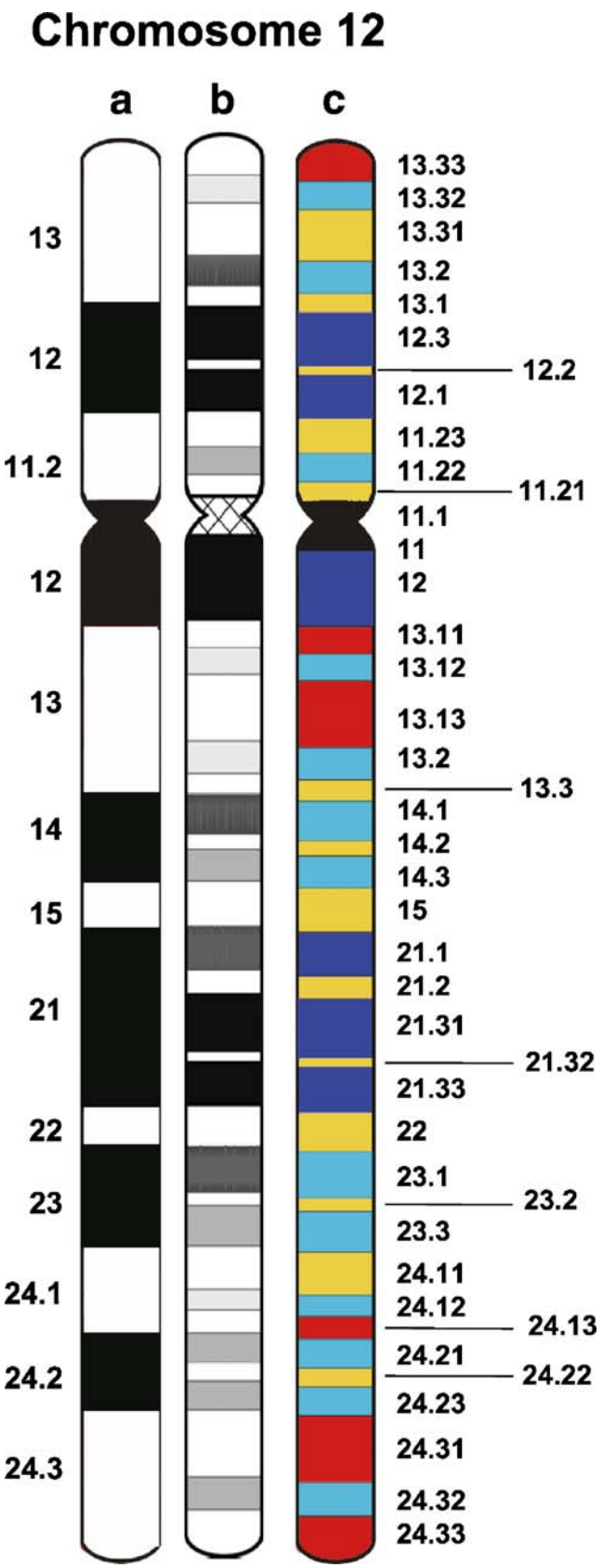

nomenclature used, but also the percentage, average GC and standard deviation in GC of chromosomal bands at a 850-band resolution, as obtained by now localizing the bands on the finished genome sequence. The relative amounts of R and G bands are 52.2% and 47.8%, respectively. The GC range of the bands is quite broad, 36.3 to 47.7%, yet there is only a small difference between the "intermediate bands" $L1^-$ and $H3^-$, which have mean GC levels of 40.1 and 41.5%, respectively. The standard deviations among bands increase from 1.09% GC for $L1^+$ bands to 3.03% GC for $H3^+$ bands, reflecting an increasing compositional heterogeneity as GC increases.

Relationships between low- and high-resolution bands Low-resolution bands unambiguously correspond, at high-resolution, both to single bands (in 39.9% of the total number, but only in 21.1% of total weight), and to multiple bands, 83.5% of which are formed by three bands (see Supplementary Table S1). Figure 1 shows the correspondence for chromosome 12 chosen as an example, by juxtaposing the low-resolution (**a**) and the high-resolution bands (**b**). The latter are presented either as the original Francke (1994) idiogram (**b**), or with the additional information derived from isochore hybridization (**c**; see the following section). Supplementary Fig. S1 provides displays similar to those of Fig. 1 for all chromosomes.

Table 2 presents the isochore hybridization properties, GC levels, and sizes of high-resolution bands from the short arm of chromosome 12 and from the long arm of chromosome 21 together with their corresponding low-resolution bands. These are two small sections of Supplementary Table S2, which presents similar data for all chromosomes. As the case of a 1:1 correspondence between low- and high- resolution bands is trivial, we will concentrate first on the majority case in which a low-resolution band is made up of three high-resolution bands (see Fig. 2), then on the other multiple bands. We will then compare the classification of the low-resolution R bands as derived from band structure (Fig. 2) with those derived from hybridization at the 400-band level, and the correspondence between the $L1^+$ and $L1^-$ bands and the G1, G2,

◀ **Fig. 1** Low (400-band) and high (850-band) resolution bands of chromosome 12. The correspondence between low- (**a**) and high-resolution (**b**) bands is unequivocally established in the literature (see Materials and methods). Panel **b** is the idiogram of Francke (1994). In the high-resolution bands of **c**, *dark blue* and *light blue* bands correspond to $L1^+$ and $L1^-$ G bands, *red and yellow bands* to $H3^+$ and $H3^-$ R bands, respectively. Each low-resolution band may correspond to one (see bands q12, q15, and q22) or, most frequently, to three high-resolution bands (see as examples bands p12, q23, and q24.1) or, more rarely, to five bands (see bands p13, q13, and q21)

Table 2 Low-resolution bands in a representative region of chromosome 12 and in the long arm of chromosome 21 are listed together with their corresponding high-resolution bands[a]

		400 band	850 band	Hybridization	GC, %	Size (Mb)	R_{tot} (Mb)	G_{tot} (Mb)
Chr. 12 p arm	**R**	**p13**	**p13.33**	**H3$^+$**	**45.8**	**3.6**		
			p13.32	*L1$^-$ (G4)*	*43.3*	*2.4*		
			p13.31	**H3$^-$**	**44.8**	**3.5**		
			p13.2	*L1$^-$ (G2)*	*37.8*	*2.0*		
			p13.1	**H3$^-$**	**42.0**	**2.9**	**10.0**	*4.4*
	G	*p12*	*p12.3*	*L1$^+$ (G1)*	*36.8*	*4.5*		
			p12.2	**H3$^-$**	**39.1**	**1.1**		
			p12.1	*L1$^+$ (G1)*	*36.7*	*4.3*	**1.1**	*8.8*
	R	**p11.2**	**p11.23**	**H3$^-$**	**39.1**	**3.8**		
			p11.22	*L1$^-$ (G3)*	*38.0*	*2.7*		
			p11.21	**H3$^-$**	**41.0**	**4.0**	**7.8**	*2.7*
Chr. 21 q arm	**R**	**q11**	**q11.2**	**H3$^-$**	**38.3**	**2.5**	**2.5**	
	G	*q21*	*q21.1*	*L1$^+$ (G1)*	*35.7*	*9.7*		
			q21.2	**H3$^-$**	**38.7**	**1.8**		
			q21.3	*L1$^+$ (G2)*	*37.5*	*3.9*	**1.8**	*13.6*
	R	**q22**	**q22.11**	**H3$^-$**	**43.7**	**2.6**		
			q22.12	*L1$^-$ (G3)*	*42.6*	*2.1*		
			q22.13	**H3$^-$**	**44.4**	**1.5**		
			q22.2	*L1$^-$ (G3)*	*42.3*	*3.9*		
			q22.3	**H3$^+$**	**50.6**	**5.5**	**9.6**	*6.0*

[a] Hybridization properties, sizes, GC levels, and total lengths of high-resolution R and G bands in each low-resolution band are shown. G and R bands nomenclature and properties are in bold and in italics, respectively. G bands are also classified G1 to G4 according to the decreasing intensity of staining (Francke 1994). R_{tot} and G_{tot} show the overall size of high-resolution R and G bands in the corresponding low-resolution bands.

G3, and G4 bands, the four decreasing intensities of G bands described by Francke (1994).

The assembly of multiple high-resolution bands in the low-resolution bands Our initial observation was that in the most common three-band case, low-resolution bands were endowed with a precise organization, in that the two "external" high-resolution bands of each triplet were G or R according to the corresponding low-resolution band, whereas the "internal" bands were always "intermediate" bands of the opposite type. More precisely, the features of the three typical high-resolution bands allow the classification of the corresponding low-resolution bands as follows (see Fig. 2). Among the G bands, the L1$^+$, L1$^{+/-}$, and L1$^-$ bands are defined as those whose outermost high-resolution G bands are both L1$^+$, or one is L1$^+$ and the other L1$^-$, or both are L1$^-$, respectively; the corresponding "internal" high-resolution bands are always intermediate H3$^-$ R bands. Likewise, among the low-resolution R bands, the H3$^+$, H3$^{+/-}$, and H3$^-$ bands comprise two outer high-resolution R bands that are both H3$^+$, or one is H3$^+$ and the other H3$^-$, or both are H3$^-$, respectively, the "internal" high-resolution bands being always intermediate L1$^-$ G bands.

Two additional points should be made here. The first one is that in terms of the total sizes they contribute, R_{850} and G_{850} bands are predominant in R_{400} and G_{400} bands, respectively (see the R_{tot} and G_{tot} columns of Table 2 and Supplementary Table S2). The second remark is that low-resolution L1$^+$, L1$^-$, H3$^+$, and H3$^-$ bands are all characterized by the predominance of the corresponding high-resolution bands. In the case of low-resolution L1$^{+/-}$ and H3$^{+/-}$ bands, L1$^+$ bands are predominant in L1$^{+/-}$ bands, whereas high-resolution H3$^+$ bands are not predominant in the H3$^{+/-}$ bands. This difference is understandable if one considers that the relative amount of L1 isochores (19%) is much larger than that of H3 isochores (3%). Moreover, the difference explains why low-resolution G bands can be accommodated in the two hybridization classes, L1$^+$ and L1$^-$, whereas low-resolution R bands belong in three different classes, H3$^+$, H3*, and H3$^-$. Indeed, the weakly hybridizing H3* largely corresponds to the H3$^{+/-}$ bands (see the following section).

In the case in which a low-resolution band corresponds to five or seven high-resolution bands (see bands 12p13, 12q13, and 12q21 of Fig. 1 for example), the external and the internal bands follow the same rule as for the three-band case, the external bands being L1$^+$, L1$^-$, H3$^+$, or H3$^-$, according to the corresponding low-resolution bands, the internal bands of the opposite type always being intermediate bands.

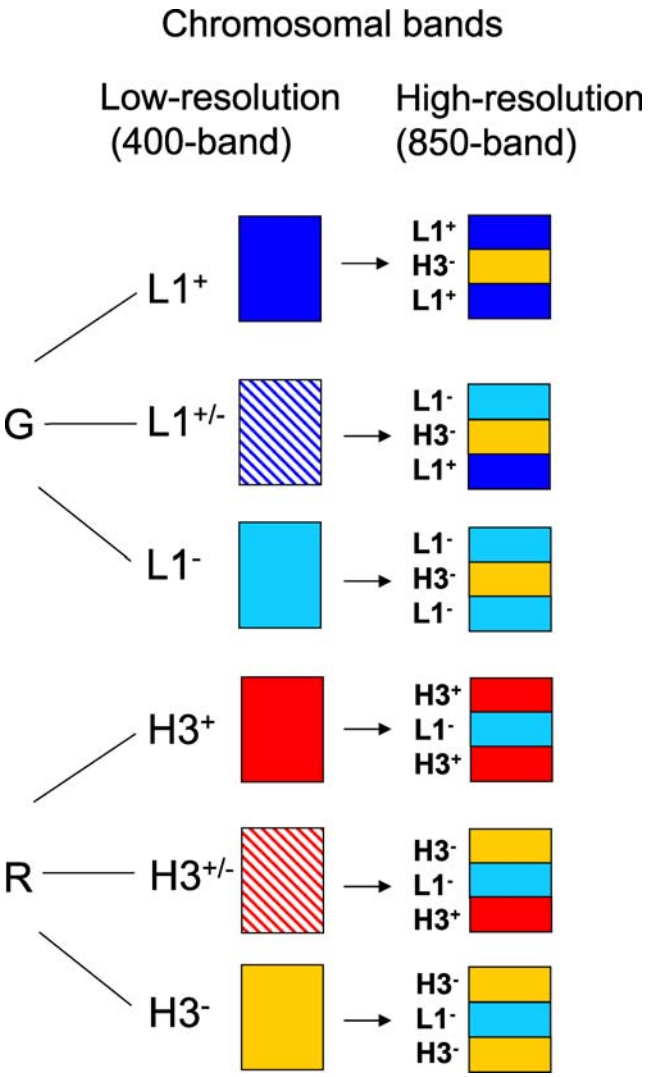

Fig. 2 Correspondence between low- and high-resolution bands. Neglecting the obvious case of a 1:1 correspondence between low- and high-resolution bands, the scheme represents the most frequent situation in which a low-resolution band corresponds to three high-resolution bands. Low-resolution $L1^+$ (*dark blue*) and $L1^{+/-}$ G bands consist of high-resolution bands in which the external bands are both $L1^+$, or one is $L1^+$ (*dark blue*) and the other $L1^-$ (*light blue*), the internal band always being $H3^-$ (*yellow*). The low-resolution $L1^-$ bands are made up of two $L1^-$ external bands and one internal $H3^-$ band. Likewise, low-resolution $H3^+$ and $H3^{+/-}$ R bands are made up of two external $H3^+$ bands, or one $H3^+$ and one $H3^-$ bands, the internal band always being $L1^-$. The low-resolution $H3^-$ bands consist of two $H3^-$ external bands and one internal $L1^-$ band

Classifications of low-resolution R bands Supplementary Table S3 lists all low-resolution bands comprising three high-resolution bands as classified according to Fig. 2. For R bands, the classification of Fig. 2 and Table S3 can be compared with (1) isochore hybridization results (Saccone et al. 1996), (2) T bands (Dutrillaux 1973), and (3) "chromatin flavors" (Holmquist 1992).

In the first case, the comparison shows that 17 out of 20 low-resolution $H3^+L1^-H3^+$ bands were seen as $H3^+$ and three as H3* by hybridization, and all 43 $H3^-L1^-H3^-$ were seen as $H3^-$. Finally, in the case of $H3^+L1^-H3^-$ bands 16 were classified as H3*, whereas eight were "misclassified" as $H3^-$ and one as $H3^+$. Overall, there is, therefore, a good agreement between the two classifications at the two resolutions.

In the second case, the $H3^+$ bands essentially correspond to the temperature-resistant T bands of Dutrillaux (1973), a subset of R bands located mainly at telomeres.

In the third case, Holmquist (1992), largely using results from Korenberg and Rykowski (1988), distinguished four "chromatin flavors": very GC-rich bands (corresponding to T bands) could be subdivided into two classes according to their high or low level of Alu sequences; likewise, relatively GC-poor bands also could be subdivided according to their high or low Alu level. We could precisely assess GC levels, Alu densities, and relative amounts of the four kinds of R bands (see Table 3) and show that the relatively GC-poor, Alu-poor class (the "mundane" flavor of Holmquist 1992) essentially corresponds to our $H3^-$ bands. Indeed these bands have very low levels of both H2 and H3 isochores, which are characterized by high Alu densities (Zerial et al. 1986; Pavliček et al. 2001). The compositional difference between Alu^+ and Alu^- very GC-rich bands is negligible, but we can confirm the different densities of Alu sequences. The Alu^- GC-rich bands are in fact all telomeric bands (see also Pavliček et al. 2001). Finally, the Alu^+ relatively GC-poor bands, a minor class, is also confirmed as having a slightly lower GC level and a high Alu level.

A comparison of Francke's G bands with hybridization bands There is a strong association between the different types of G bands (G1, G2, G3, and G4) of Francke (1994) and GC level, as found by hybridization with the GC-poorest L1 DNA (Federico et al. 2000). The mean GC of the bands in G1 is 36.5%, in G2 37.7%, in G3 39.9%, and in G4 41.5%. Thus, $L1^+$ bands in the human genome are predominantly G1 bands (see Table 4), and almost all of them are either G1 or G2 (102 vs only 4). As shown in the full contingency Table 4, the converse situation also holds, although it is not quite as striking. Thus, $L1^-$ bands are indeed predominantly G3 or G4 (204 vs 68 bands, but there is not much difference between G3 and G4 in terms of hybridization, as comparable numbers of $L1^-$ (or $L1^+$) bands and very similar observed/expected ratios are found in both categories. Supplementary Table S4 shows the counts and observed/expected ratios when the bands are classified according to their GC (as determined by the present map) instead of their hybridization.

Compositional contrasts The compositional proximity of "intermediate bands", $L1^-$ and $H3^-$ (in spite of the former being G bands and the latter R bands; see Table 1), as well

Table 3 Alu density, base composition, frequency, length, and hybridization properties of the four classes of R bands proposed by Holmquist (1992) in the human genome[a]

R bands	Alu density[(a)]	GC, %	Number of bands	H3+	H3*	H3$^-$	Size, Mb	H3$^+$, Mb	H3*, Mb	H3$^-$, Mb
Mundane R	455.39	41.7	98	0	3	95	789.7	0	16.9	772.8
Alu$^-$ GC$^+$	463.86	46.0	14	7	7	0	199.4	100.5	98.9	0
Alu$^+$ GC$^-$	782.64	44.3	7	0	3	4	41.5	0	19.8	21.7
Alu$^+$ GC$^+$	716.85	46.5	27	16	8	3	398.1	276.6	64.1	20.9

[a] Alu density was calculated as the number of Alu sequences per Mb for each R band. The number given reports the mean of those densities in each class of R bands. To allow comparison with Holmquist (1992) the band definition of the The National Foundation (1972) was used; see also Bostock and Sumner (1978).

as the existence of intermediate G bands that are GC-richer than R bands, suggested that base composition per se could not be the reason for a band to be G or R (Saccone et al. 2001). Indeed, the data of Fig. 3 show that the reason is rather the compositional contrast with flanking bands, as each band (at both low and high resolutions) is flanked by two adjacent bands that are both lower in GC in the case of R bands, or both higher in GC in the case of G bands. In a minority of isochores representing 22.4% of the genome, however, one flanking isochore was higher, the other one lower in GC (see Fig. 3c). These isochores corresponded to "transition isochore bands" between GC-richer and GC-poorer isochore bands (see Costantini et al. 2006).

GC levels of high resolution bands While the average GC levels and standard deviations of L1$^+$, L1$^-$, H3$^-$, and H3$^+$ bands were already presented in Table 1, Fig. 4 presents the compositional distributions of the four classes of bands. The most remarkable feature is the extensive compositional overlap of the "intermediate bands" L1$^-$ and H3$^-$ and the lack of overlap of L1$^+$ and H3$^+$ bands.

Sizes of high-resolution bands While the size distributions of "intermediate bands" L1$^-$ and H3$^-$ were relatively narrow and showed a large overlap, the L1$^+$ and the H3$^+$ bands showed very broad size distributions, and the L1$^+$ bands reached higher sizes (Fig. 5a,b). In other words, size distributions were distinctly different for these two groups of bands. The corresponding size distributions of bands, as derived from the idiogram of Francke (1994; Fig. 5b), were in reasonable concordance with those obtained via sequence data, although with a notable and systematic exception for the L1$^+$ bands, which have in fact longer sequences and, therefore, a higher compaction (see also Fig. 6).

A comparison of chromosomal bands Figure 6a shows the idiogram of Francke (1994) incorporating our compositional (hybridization) map (Federico et al. 2000) for the long arm of chromosome 21, chosen as an example, while Fig. 6b also shows the locations of the high-resolution bands along the sequence as determined in the present study. A comparison of the results presented in Fig. 6a,b shows differences in both the sizes and the precise locations of bands. The first effect is expected as a result of compaction phenomena (see above), the second as a result of both compaction and the less precise assessment of band borders by cytogenetics. Figure 6c shows the isochores of chromosome 21 to illustrate how the borders of high-resolution bands were defined on the basis of the isochore map of Costantini et al. (2006). Finally, Fig. 6d displays the results of Furey and Haussler (2003) for comparison (see Discussion).

Isochores and chromosomal bands At low and high resolutions, the compositional contrast responsible for chromosomal bands implies GC jumps (see Fig. 3), which can be easily viewed on GC profiles. In recent work (Costantini et al. 2006), we provided an isochore map defined at a 100-kb level, below which the GC profile becomes turbulent owing to the contribution of specific sequences (exons, introns, CpG islands, interspersed

Table 4 Association between the bands of Francke (1994) and the hybridization bands[a]

Bands			Number of bands hybridized with L1 DNA (and observed/expected ratios)	
Type	Mean GC, %	Number	L1$^+$	L1$^-$
G1	36.5	79	*67 (3.02)*	12 (0.21)
G2	37.7	91	*35 (1.37)*	56 (0.85)
G3	39.9	120	4 (0.12)	*116 (1.34)*
G4	41.5	89	0 (0.00)	*89 (1.39)*
		379	106	273

[a] The contingency table shows counts and observed/expected ratios (in brackets) for L1$^+$ and L1$^-$ bands and their association with the four classes of bands. Expected counts are those if no association were present (p of chi-squared test $<10^{-43}$). Values in italics indicate observed/expected >1.2.

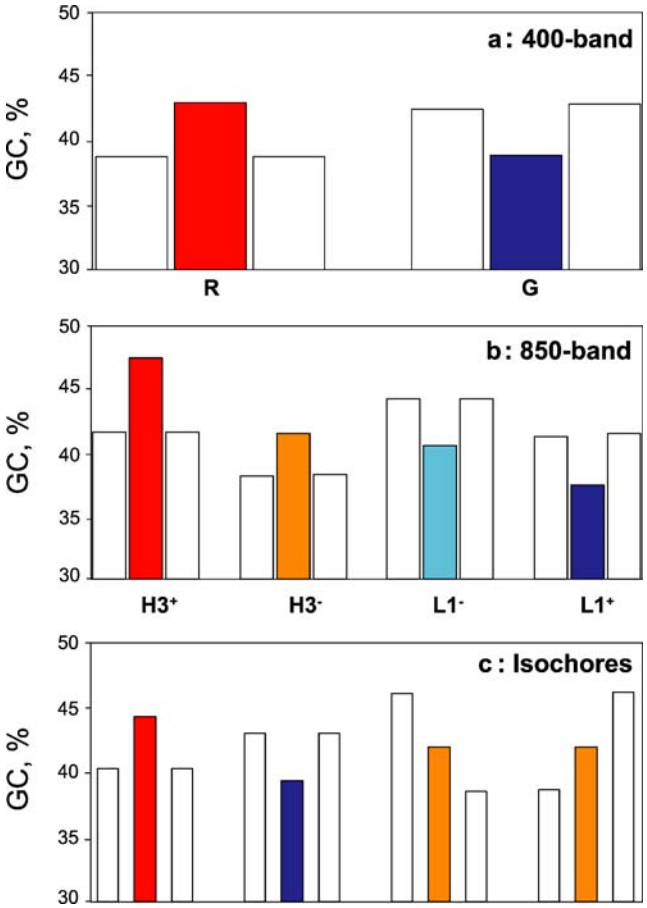

Fig. 3 Compositional contrasts with flanking bands. The diagram shows the average GC contrasts with preceding and following bands: (**a**) at low resolution, (**b**) at high resolution, and (**c**) at the isochore (or highest) resolution. At 400-band and 850-band resolutions, each band is flanked by two adjacent bands that were either both lower in GC (in the case of R bands) or higher in GC (in the case of G bands). Also at the isochore resolution, $H3^+$ isochores are always flanked by GC-poorer isochores, and $L1^+$ isochores are always flanked by GC-richer isochores, as expected; in several cases, $L1^-$ and $H3^-$ bands exhibit "transition isochores", where one flanking isochore is higher, the other one being lower (see also Fig. S1 of Costantini et al. 2006)

repeats, etc.). Most interestingly, isochores are associated in blocks that correspond to the high-resolution bands according to a specific rule, which is that each isochore is predominantly flanked by isochores of the nearest compositional family (see Fig. 7). This made it possible to localize the compositional changes, namely, the borders, between high-resolution bands at the isochore level, i.e., at a definition of 100 kb, a value well below that (2–3 Mb) provided by cytogenetics. In turn, this led to the same level of definition for the borders between low-resolution bands. Interestingly, the average ΔGC or compositional jump increased from 3.9 to 4.1% and to 4.4% when taking into consideration isochores, high-resolution and low-resolution bands (see Fig. 8), respectively. In other words, among the compositional jumps between the isochores, the slightly larger ones are those that separate high-resolution bands, and among the compositional jumps between high-resolution bands, the larger ones are those that separate low-resolution bands.

Discussion

We will not go into a historical discussion of chromosomal banding, a subject on which an abundant literature is available, but will confine ourselves to a discussion of the assembly rules underlying the structure of chromosomal bands and to a comparison of our results with those of previous results.

As far as the assembly rules of chromosomal bands are concerned, it should be stressed that the correspondence of high-resolution (850-band) and low-resolution (400) bands is generally agreed upon and is independent of the precise size and precise chromosomal location of the bands. The rules that have emerged from the present work are the following. In the predominant case in which each low-resolution band consists of several (generally three) high-resolution bands, (a) the external high-resolution bands are always G or R according to whether the corresponding low-resolution band is G or R, respectively; (b) the internal high-resolution bands of the opposite type are always intermediate bands; (c) the predominant high-resolution bands typically belong to the same type as the corresponding low-resolution band. If we now consider high-resolution bands, we find that their isochores are flanked by isochores of the compositionally closest family. This leads to the formation of isochore blocks that make up the high-resolution bands. Finally, a general rule is that the compositional contrasts rather than the absolute

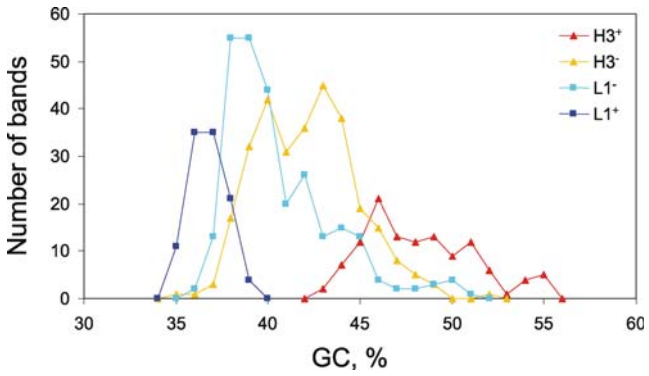

Fig. 4 Compositional distributions of high-resolution bands on human chromosomes. The histograms show the GC distribution (by number) of bands at high resolution, as pooled in bins of 1% GC. $L1^+$ and $H3^+$ (bands) show no compositional overlap, whereas the "intermediate bands", $L1^-$ and $H3^-$, show an extensive overlap

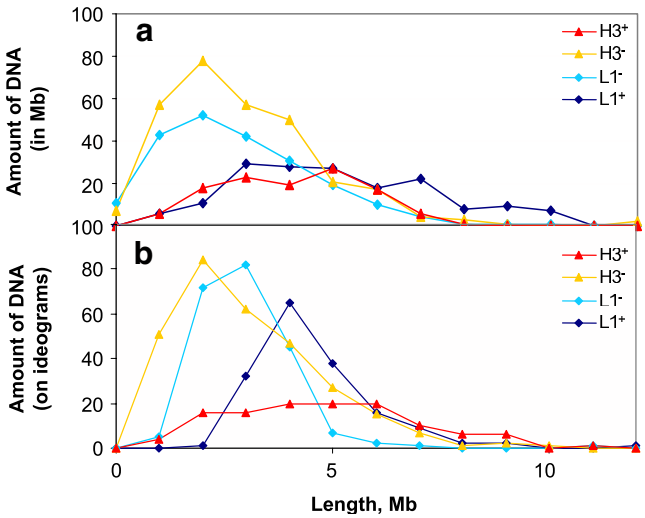

Fig. 5 Compositional distributions of sizes of different classes of high-resolution bands on human chromosomes. The histograms in **a** represent length distributions for the high-resolution (850-band) chromosomal bands, classified as $L1^+$, $L1^-$, $H3^-$, and $H3^+$. The histograms in **b** show the lengths of the same cytogenetic bands as reported in the original digitized idiograms of Francke (1994). To allow comparison of the two sets of distributions, cytogenetic band lengths in the digitized idiograms were converted to their equivalents in Mb, by equating the total lengths for all the chromosomes' euchromatic (sequenced and aligned) DNA

compositional levels determine the type of bands at both resolution levels.

A comparison of our results with previous data as obtained for low-resolution R bands (Dutrillaux 1973; Korenberg and Rykowski 1988; Holmquist 1992) and for high-resolution G bands (Francke 1994) stresses a basic agreement, which is really remarkable in view of the limitations of cytogenetics and of the fact that those investigations were carried out in the total absence of genome sequences. The comparisons were presented in the Results section.

To compare our results with another recent band localization, we chose the map of Furey and Haussler (2003), which is incorporated into the UCSC database and was an obvious choice for a more detailed comparison with ours. Indeed only compositional information of bulk DNA was used throughout our map's construction and no reference was made to clone hybridization data or to sequence landmarks such as genes. In contrast, the map of Furey and Haussler (2003) was derived via an independent route that did not use GC information but instead used high-quality clone localizations. This map is publicly available in precise coordinates along the finished sequence. In addition, it respects the classical numbers of bands (Francke 1994) on each chromosome arm and was obtained using 100-kb windows in a similar way as we have done in this study.

We compared the two maps directly by aligning them (see Fig. 6), and found that band boundary estimates rarely deviate dramatically, so that there is a reasonable correlation (R=0.62) between the lengths of corresponding bands. There is, however, a difference in that Furey and Haussler's procedure did not lead to a regularly alternating sequence of GC-richer and GC-poorer bands. Indeed, in our case, flanking bands are always higher or lower than the internal band, whereas in the case of Furey and Haussler (2003), one flanking band is often lower and the other one is higher (for such a ladder shape, see bands 21q21.2–22.12).

Although the alternating compositional pattern that we observe is based on GC, clone hybridization estimates alone might, in principle, have led to a similar pattern, without the need for compositional information. Figure 6 strongly suggests that this is not the case. In other words, explicit GC information is needed to reveal the characteristic alternating pattern. Supplementary information discusses the cross-validation of our map with the data from clone hybridization.

In conclusion, the major results obtained in the present investigation were the following: (1) finding the "rules" that underlie the structure of chromosomal bands from the low- to the high- and to the highest resolution, to form the nested

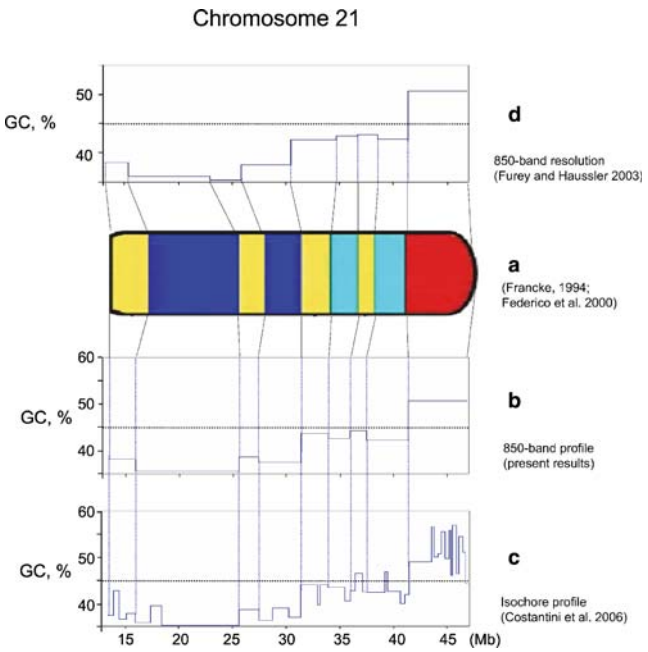

Fig. 6 Comparison between cytogenetic bands, hybridization results, and sequence GC levels. Human chromosome 21 is displayed as an example (see Table 2 for details). *A* shows the high-resolution idiogram of Francke (1994) incorporating the hybridization results of Federico et al. (2000): $L1^+$ (*dark blue*), $L1^-$ (*light blue*), $H3^-$ bands (*yellow*) and $H3^+$ (*red*). Assessing GC variation at the sequence level makes it possible to locate the compositional changes between adjacent high-resolution bands on the chromosome, at a resolution of 100 kb, on the basis of GC jumps. In the resulting GC profile *B*, horizontal stretches represent the bands at an 850-band resolution. The corresponding isochore profile is reported in *C*. The top profile (*D*) is from the map of Furey and Haussler (2003)

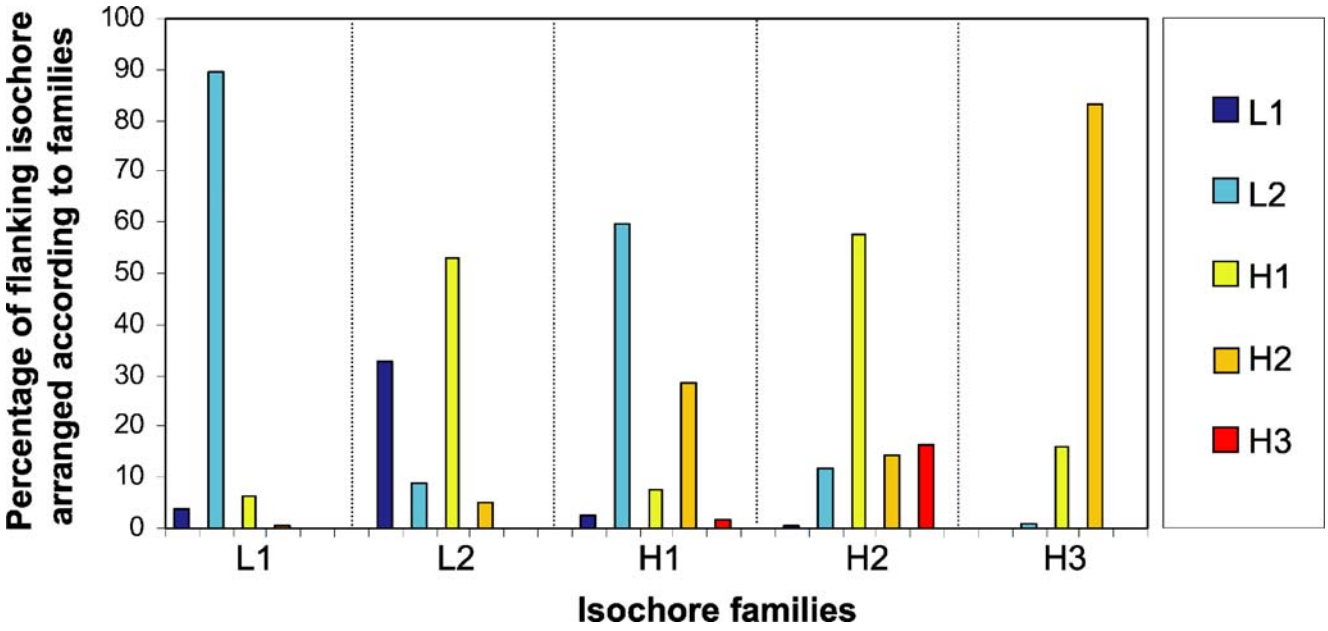

Fig. 7 Flanking isochores. The histogram shows (*vertical axis*) the percentages of flanking isochores as arranged according to isochore families. The *horizontal axis* shows the isochore family of the "internal" isochores. The rare cases in which an isochore is flanked by another isochore of the same family occur because each of the isochore families spans an appreciable range of GC, up to 7% for H2 (Costantini et al. 2006), whereas adjacent isochores can differ by as little as 2% GC. These rare cases never involve two entire bands at the 850-band resolution

mosaic structure of chromosomes. This first point provides the best evidence for a precise order in the structuring of chromosomal bands, thus vindicating more than a century later the view of Rabl (1885) that "order must be" in chromosomes; (2) mapping borders of chromosomal bands, to the nearest 100 kb, on the basis of the isochore map of Costantini et al. (2006); (3) explaining the molecular basis for cytogenetic chromosomal banding. Indeed, we have shown that chromosome bands can be defined on the basis of compositional properties alone, and that the different staining intensities of high-resolution G bands (Francke 1994) are correlated with GC levels. Then, the only plausible explanation is that chromosomal bands are due to compositional properties and, ultimately, to the underlying chromosome bands' isochore patterns.

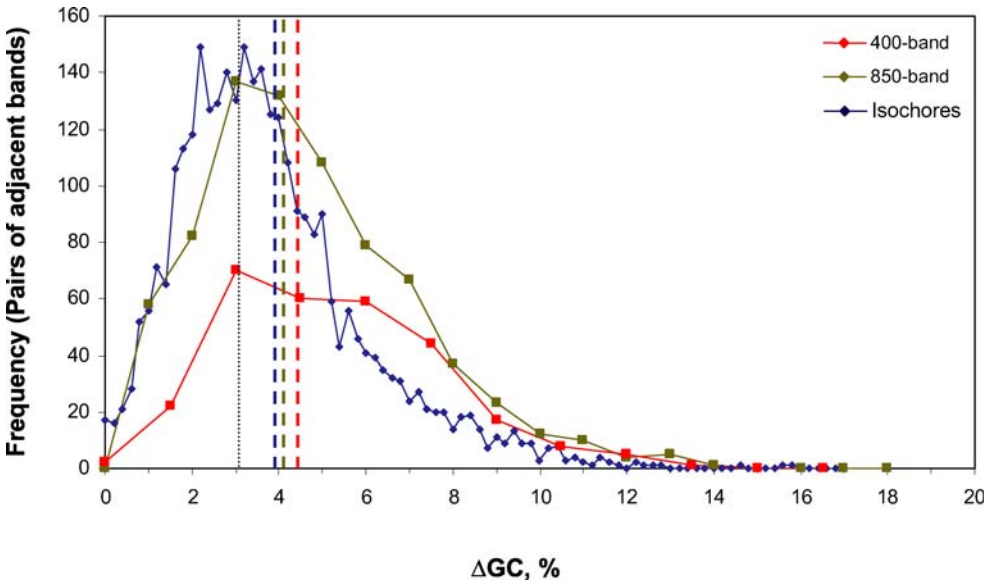

Fig. 8 ΔGC distribution of adjacent isochores. The frequency plot shows the differences (jumps) in GC between adjacent low-resolution bands (*red line*), high-resolution bands (*green line*), and isochores (*blue line*). The modal jumps in GC are all approximately 3% (*thin dashed line*). The mean jumps (by number) are reported for the three levels of band resolutions (3.9% for isochores, 4.1% for 850 bands, and 4.5% for 400 bands, represented in the plot by *blue*, *green*, and *red dashed lines*, respectively)

References

Aota S, Ikemura T (1986) Diversity in G+C content at the third position of codons in vertebrate genes and its cause. Nucleic Acids Res 14:6345–6355

Bailly S, Guillemin C, Labrousse M (1973) Comparison du nombre et de la position des zones spécifiques révélées sur les chromosomes mitotiques de l'Amphibien Urodéle *Pleurodeles waltlii Michah* par les techniques de coloration au colorant de Giemsa et à la moutarde de quinacrine. CR Acad Sci Paris 276:1867–1869

Bernardi G (1989) The isochore organization of the human genome. Ann Rev Genet 23:637–661

Bernardi G (2004, reprinted in 2005) Structural and evolutionary genomics. Natural selection in genome evolution. Elsevier, Amsterdam, The Netherlands

Bernardi G, Olofsson B, Filipski J, Zerial M, Salinas J, Cuny G, Meunier-Rotival M, Rodier F (1985) The mosaic genome of warm-blooded vertebrates. Science 228:953–957

Bostock CJ, Sumner AT (1978) The eukaryotic chromosome. North-Holland, Amsterdam NewYork Oxford

Caspersson T, Farber S, Foley GE, Kudynowski J, Modest EJ, Simonsson E, Wagh U, Zech L (1968) Chemical differentiation along metaphase chromosomes. Exp Cell Res 49(1):219–222

Caspersson T, Zech L, Johansson C (1970) Differential binding of alkylating fluorochromes in human chromosomes. Exp Cell Res 60:315–319

Claussen U, Lehrer H, Hliscs R, Kuechler A, Weise A, Liehr T (2005) The splitting of human chromosome bands into sub-bands. European Human Genetics Conference 2005 (http://www.eshg.org/eshg2005)

Comings DE (1978) Mechanisms of chromosome banding and implications for chromosome structure. A Rev Genet 12:25–46

Corneo G, Ginelli E, Soave C, Bernardi G (1968) Isolation and characterization of mouse and guinea pig satellite DNA's. Biochemistry 7:4373–4379

Costantini M, Clay O, Auletta F, Bernardi G (2006) An isochore map of human chromosomes. Genome Res 16:536–541

Cuny G, Soriano P, Macaya G, Bernardi G (1981) The major components of the mouse and human genomes: preparation, basic properties and compositional heterogeneity. Eur J Biochem 111:227–233

De Sario A, Geigl EM, Palmieri G, D'Urso M, Bernardi G (1996) A compositional map of human chromosome band Xq28. Proc Natl Acad Sci USA 93:1298–1302

De Sario A, Roizès G, Allegre N, Bernardi G (1997) A compositional map of the cen-q21 region of human chromosome 21. Gene 194:107–113

Dev VG, Warburton D, Miller OJ (1972) Giemsa banding of chromosomes. Lancet 1:1285

Dutrillaux B (1973) Nouveau système de marquage chromosomique: les bandes T. Chromosoma 41:395–402

Dutrillaux B, Lejeune J (1971) A new technique of analysis of the human karyotype. C R Acad Sci Hebd Seances Acad Sci D 272:2638–2640

Dutrillaux B, Rethorè MO, Lejeune J (1975) Comparison of the karyotype of the orangutan (*Pongo pygmaeus*) to those of man, chimpanzee, and gorilla. Ann Genet 18:153–161

Ellison JR, Barr HJ (1972) Quinacrine fluorescence of specific chromosome regions. Late replication and high A:T content in *Samoia leonensis*. Chromosoma 36(4):375–390

Federico C, Andreozzi L, Saccone S, Bernardi G (2000) Gene density in the Giemsa bands of human chromosomes. Chromosome Res 8:737–746

Filipski J, Thiery JP, Bernardi G (1973) An analysis of the bovine genome by $Cs_2SO_4^-Ag^+$ density gradient centrifugation. J Mol Biol 80:177–197

Francke U (1994) Digitized and differentially shaded human chromosome idiograms for genomic applications. Cytogenet Cell Genet 6:206–219

Furey TS, Haussler D (2003) Integration of the cytogenetic map with the draft human genome sequence. Hum Mol Genet 12:1037–1044

Furst A, Brown EH, Braunstein JD, Schildkraut CL (1981) Alpha-globulin sequences are located in a region of early-replicating DNA in murine erythroleukemia cells. Proc Natl Acad Sci USA 78:1023–1027

Goldman MA, Holmquist GP, Gray MC, Caston LA, Nag A (1984) Replication timing of genes and middle repetitive sequences. Science 224:686–692

Holmquist GP (1992) Chromosome bands, their chromatin flavors, and their functional features. Am J Hum Genet 51:17–37

Holmquist G, Gray M, Porter T, Jordan J (1982) Characterization of Giemsa dark- and light-band DNA. Cell 31(1):121–129

Ikemura T, Aota S (1988) Alternative chromatic structure at CpG islands and quinacrine-brightness of human chromosomes. Global variation in G+C content along vertebrate genoma DNA. Possible correlation with chromosome band structures. J Mol Biol 60:909–920

ISCN (1981) An international system for human cytogenetic nomenclature—high-resolution banding. Cytogenet Cell Genet 31:1–23

ISCN (2005) An international system for the human cytogenetic nomenclature. In: Schweizer LG, Tommerup N (eds). Karger, Basel

Korenberg JR, Engels WR (1978) Base ratio, DNA content, and quinacrine brightness of human chromosomes. Proc Natl Acad Sci USA 75:3382–3386

Korenberg JR, Rykowski MC (1988) Human genome organization: Alu, lines, and the molecular structure of metaphase chromosome bands. Cell 53(3):391–400

Lehrer H, Weise A, Michel S, Starke H, Mrasek K, Heller A, Kuechler A, Claussen U, Liehr T (2004) The hierarchically organized splitting of chromosome bands into sub-bands analyzed by multicolor banding (MCB). Cytogenet Genome Res 105:25–28

Lima-de-Faria A, Isaksson M, Olsson E (1980) Action of restriction endonucleases on the DNA and chromosmes of *Muntiacus muntjak*. Hereditas 92:267–273

Macaya G, Thiery JP, Bernardi G (1976) An approach to the organization of eukaryotic genomes at a macromolecular level. J Mol Biol 108:237–254

Pachmann U, Rigler R (1972) Quantum yield of acridines interacting with DNA of defined sequence. A basis for the explanation of acridine bands in chromosomes. Exp Cell Res 72(2):602–608

Pavliček A, Jabbari K, Pačes J, Pačes V, Hejnar J, Bernardi G (2001) Similar integration but different stability of Alus and LINEs in the human genome. Gene 276:39–45

Rabl C (1885) Über Zelltheilung. Morphologisches Jahrbuch 10:214–230

Rooney ED (ed) (2001) Human cytogenetics: constitutional analysis. Oxford University Press, Oxford

Saccone S, De Sario A, Della Valle G, Bernardi G (1992) The highest gene concentrations in the human genome are in telomeric bands of metaphase chromosomes. Proc Natl Acad Sci USA 89:4913–4917

Saccone S, De Sario A, Wiegant J, Raap AK, Della Valle G, Bernardi G (1993) Correlations between isochores and chromosomal bands in the human genome. Proc Natl Acad Sci USA 90:11929–11933

Saccone S, Cacciò S, Kusuda J, Andreozzi L, Bernardi G (1996) Identification of the gene-richest bands in human chromosomes. Gene 174:85–94

Saccone S, Federico C, Solovei I, Croquette MF, Della Valle G, Bernardi G (1999) Identification of the gene-richest bands in human prometaphase chromosomes. Chromosome Res 7:379–386

Saccone S, Pavliček A, Federico C, Pačes J, Bernardi G (2001) Gene, isochores and bands in human chromosomes 21 and 22. Chromosome Res 9:533–539

Saccone S, Federico C, Andreozzi L, D'Antoni S, Bernardi G (2002) Localization of the gene-richest and the gene-poorest isochores in the interphase nuclei of mammals and birds. Gene 300:169–178

Schimke RT (1982) Gene amplification. Cold Spring Harbor, New York, NY, USA

Schmid M (1978) Chromosome banding in amphibians. Chromosoma 68:131–148

Schweizer D (1977) R-banding produced by DNase I digestion of chromomycin-stained chromosomes. Chromosoma 64:117–124

Stock AD, Mengden GA (1975) Chromosomes banding pattern conservatism in birds and non-homology of chromosome banding patterns between birds, turtles, snakes and amphibians. Chromosoma 50:69–77

The National Foundation (1972) Standardization in human cytogenetics. Birth defects. In: Proceedings of Paris Conference 1971, Original article series, vol 8, no 7; also in Cytogenetics 11:317–362

Thiery JP, Macaya G, Bernardi G (1976) An analysis of eukaryotic genomes by density gradient centrifugation. J Mol Biol 108:219–235

Weisblum B, de Haseth PL (1972) Quinacrine, a chromosome stain specific for deoxyadenylate-deoxythymidylaterich regions in DNA. Proc Natl Acad Sci USA 69:629–632

Wurster-Hill DH, Gray CW (1979) The interrelationship of chromosome banding patterns in procyonids, viverrids, and felids. Cytogenet Cell Genet 15:306–331

Yunis JJ (1976) High resolution of human chromosomes. Science 191:1268–1270

Yunis JJ (1981) Mid-prophase human chromosome. The attainment of 2,000 bands. Hum Genet 56:291–298

Yunis JJ, Tsai MY, Willey AM (1977) Molecular organization and function of the human genome. In: Yunis JJ (ed) Molecular structure of human chromosomes. Academic, New York, NY

Zerial M, Salinas J, Filipski J, Bernardi G (1986) Gene distribution and nucleotide sequence organization in the human genome. Eur J Biochem 160:479–485